THE JOURNAL OF BIOLOGICAL CHEMISTRY VOL. 285, NO. 29, pp. 22696–22705, July 16, 2010

Structural Basis for Conformational Dynamics of GTP-bound Ras Protein*[S]

Received for publication, March 19, 2010, and in revised form, April 28, 2010 Published, JBC Papers in Press, May 17, 2010, DOI 10.1074/jbc.M110.125161

Fumi Shima[‡1], Yuichi Ijiri[‡1], Shin Muraoka[‡§1], Jingling Liao[‡1], Min Ye[‡], Mitsugu Araki[¶], Kousuke Matsumoto[‡], Naoki Yamamoto[¶], Takeshi Sugimoto[‡], Yoko Yoshikawa[‡], Takashi Kumasaka[‖], Masaki Yamamoto[§], Atsuo Tamura[¶], and Tohru Kataoka[‡2]

From the [‡]Division of Molecular Biology, Department of Biochemistry and Molecular Biology, Kobe University Graduate School of Medicine, 7-5-1 Kusunoki-cho, Chuo-ku, Kobe 650-0017, Japan, the [¶]Department of Chemistry, Kobe University Graduate School of Science, 1-1 Rokkodai, Nada-ku, Kobe 657-8501, Japan, the [‖]Japan Synchrotron Radiation Research Institute, 1-1-1 Kouto, Sayo-cho, Sayo-gun, Hyogo 679-5198, Japan, and the [§]RIKEN SPring-8 Center, 1-1-1 Kouto, Sayo-cho, Sayo-gun, Hyogo 679-5148, Japan

Ras family small GTPases assume two interconverting conformations, "inactive" state 1 and "active" state 2, in their GTP-bound forms. Here, to clarify the mechanism of state transition, we have carried out x-ray crystal structure analyses of a series of mutant H-Ras and M-Ras in complex with guanosine 5′-(β,γ-imido)triphosphate (GppNHp), representing various intermediate states of the transition. Crystallization of H-RasT35S-GppNHp enables us to solve the first complete tertiary structure of H-Ras state 1 possessing two surface pockets unseen in the state 2 or H-Ras-GDP structure. Moreover, determination of the two distinct crystal structures of H-RasT35S-GppNHp, showing prominent polysterism in the switch I and switch II regions, reveals a pivotal role of the guanine nucleotide-mediated interaction between the two switch regions and its rearrangement by a nucleotide positional change in the state 2 to state 1 transition. Furthermore, the ^{31}P NMR spectra and crystal structures of the GppNHp-bound forms of M-Ras mutants, carrying various H-Ras-type amino acid substitutions, also reveal the existence of a surface pocket in state 1 and support a similar mechanism based on the nucleotide-mediated interaction and its rearrangement in the state 1 to state 2 transition. Intriguingly, the conformational changes accompanying the state transition mimic those that occurred upon GDP/GTP exchange, indicating a common mechanistic basis inherent in the high flexibility of the switch regions. Collectively, these results clarify the structural features distinguishing the two states and provide new insights into the molecular basis for the state transition of Ras protein.

Small GTPases Ras (H-Ras, K-Ras, and N-Ras) are the products of the *ras* proto-oncogenes and presumed to be some of the most promising targets for anti-cancer drug development because of their high frequency of mutational activation in a variety of human cancers (1). Ras functions as a molecular switch by cycling between GTP-bound active and GDP-bound inactive forms in intracellular signaling pathways controlling cell growth and differentiation. Conversion between the GDP-bound and the GTP-bound forms is controlled by guanine nucleotide exchange factors and GTPase-activating proteins (2, 3). Ras comprises the Ras family of small GTPases together with a number of its relatives, including Rap1, Rap2, R-Ras, R-Ras2/TC1, M-Ras/R-Ras3, etc. (1). X-ray crystallographic and NMR analyses of H-Ras and Rap1A, alone or in complex with their effectors, revealed that the exchange of GTP for GDP results in allosteric conformational changes in two adjacent regions, termed switch I (residues 32–38) and switch II (residues 60–75), and enables Ras to execute downstream signaling through direct interaction with its effectors, such as Raf kinases and phosphoinositide 3-kinases (2, 3).

Recent ^{31}P NMR spectroscopic studies on Ras unveiled its novel structural feature, the conformational dynamics in the GTP-bound form (4). H-Ras and K-Ras in complex with Mg^{2+} and a non-hydrolyzable GTP analogue, GppNHp,[3] exhibit equilibrium between two distinct conformational states, state 1 and state 2, which are characterized by different chemical shift values for the resonance of the nucleotide phosphorus atoms of the α- and γ-phosphate groups. The interconversion between the two states occurs on a millisecond time scale and appears to be a general property shared by members of the Ras family small GTPases irrespective of the nature of the bound guanine nucleotide triphosphate: GTP, GppNHp, or GTPγS (5–8). However, the state distribution exhibited a great variation among various GTPase species; H-Ras-GppNHp and Rap2A-GppNHp predominantly assume state 2, whereas M-Ras-GppNHp predominantly assumes state 1 (7). Because association of H-Ras-GppNHp with its various effectors induced a shift of the equilibrium toward state 2, state 1 and state 2 were presumed to represent the inactive and active conformations, respectively (4, 9–11). Although state 2 corresponds to the structure solved

* This work was supported by Grants-in-Aid for Scientific Research in Priority Areas 17014061 and 18057014, and Global Centers of Excellence Program A08 from the Ministry of Education, Science, Sports, and Culture of Japan and by National Institute of Biomedical Innovation Grant for the Program for Promotion of Fundamental Studies of Health Sciences 06-3.

[S] The on-line version of this article (available at http://www.jbc.org) contains supplemental Tables 1–3 and Figs. 1–5.

The atomic coordinates and structure factors (codes 3KKM, 3KKN, 3KKO, 3KKP, and 3KKQ) have been deposited in the Protein Data Bank, Research Collaboratory for Structural Bioinformatics, Rutgers University, New Brunswick, NJ (http://www.rcsb.org/).

[1] These authors contributed equally to this work.

[2] To whom correspondence should be addressed. Tel.: 81-78-382-5380; Fax: 81-78-382-5399; E-mail: kataoka@people.kobe-u.ac.jp.

[3] The abbreviations used are: GppNHp, guanosine 5′-(β,γ-imido)triphosphate; GTPγS, guanosine 5′-3-*O*-(thio)triphosphate; PEG, polyethylene glycol; RasWT, wild type Ras; r.m.s., root mean square; MES, 4-morpholineethanesulfonic acid.

with the crystal of H-Ras-GppNHp alone (Protein Data Bank entries 1CTQ and 5P21) or in complex with the effectors (12–14), the tertiary structure corresponding to state 1 remained to be determined. Recently, we succeeded in solving the first tertiary structure of state 1 by crystallizing M-Ras-GppNHp (15). The state 1 structure is distinguished from state 2 by the loss of the direct and Mg^{2+}-coordinated indirect interactions of Thr-45 of M-Ras (corresponding to Thr-35 of H-Ras) with the γ-phosphate of GppNHp, which causes marked deviation of the switch I loop away from the guanine nucleotide and conformational instability of the switch I loop. The result is consistent with the mechanism for the ^{31}P NMR chemical shift changes accompanying the state transition; the distance of the γ-phosphate from the aromatic ring of Tyr-32 in switch I of H-Ras, which exerts a "ring current shift" effect, is a major determinant of the γ-phosphate chemical shift change. Another Tyr residue in the switch regions, Tyr-64 in switch II, is too far away to exert a significant effect. This indicates that the interconversion between state 1 and state 2 is mainly accounted for by reversible engagements of the Thr-35/45-γ-phosphate interaction, taken together with the result of past electron spin resonance studies on the Mg^{2+}-binding site of H-Ras, showing the transient nature of the coordination of Thr-35 to the γ-phosphate (16, 17). Moreover, the marked deviation of the switch I loop away from the guanine nucleotide results in formation of a surface pocket surrounded by the guanine nucleotide and the two switch regions in the M-Ras-GppNHp structure.

In the present study, we succeed in solving the first complete tertiary structure of H-Ras-GTP state 1, possessing two surface pockets, through crystallization of H-RasT35S-GppNHp. Moreover, determination of two distinct crystal structures of H-RasT35S-GppNHp enables us to clarify the structural features distinguishing the two states and gain new insights into the molecular mechanism for the state transition, which is also backed by structural analysis of M-Ras mutants representing various state intermediates. Further, the significance of the structural information on H-Ras-GTP state 1, especially on its surface pockets, in structure-based drug design of Ras inhibitors will be discussed.

EXPERIMENTAL PROCEDURES

Protein Purification—Human H-RasT35S (residues 1–166), mouse M-RasP40D (residues 1–178), M-RasL51R (residues 1–178), and M-RasP40D/D41E/L51R (residues 1–178) were expressed as fusions with glutathione *S*-transferase in *Escherichia coli* using pGEX-6P-1 vector (GE Healthcare), immobilized on glutathione-agarose, and eluted by cleavage with PreScission protease (GE Healthcare). Mouse M-RasD41E (residues 1–178), M-RasP40D/D41E (residues 1–178), and M-RasP40D/D41E/L51R/F74Y/E79D (residues 1–178) were expressed with an N-terminal His_6 tag in *E. coli* using pQE30 vector (Qiagen, Valencia, CA) and purified by affinity chromatography on Ni^{2+}-NTA-agarose (Qiagen). After further purification by ion exchange chromatography to a final purity of >95%, they were loaded with GppNHp and used for crystallization or NMR spectroscopy as described before (10). Human c-Raf-1 Ras-binding domain (residues 51–130) was purified as described (7).

NMR Spectroscopy—^{31}P NMR spectra were recorded in the presence or absence of c-Raf-1 Ras-binding domain on a Brucker AVANCE-500 NMR spectrometer (15). The ^{31}P spectra were referenced as described before (10).

Crystallization of Ras Proteins in Complex with Mg^{2+} and GppNHp—H-RasT35S-GppNHp was dissolved in buffer 1 (40 mM Tris-HCl, pH 7.4, 50 mM NaCl, and 5 mM $MgCl_2$) and buffer 2 (40 mM Tris-HCl, pH 7.4, 50 mM NaCl, 5 mM $MgCl_2$, and 7% DMSO), yielding protein solution 1 and 2, respectively. Crystals of H-RasT35S-GppNHp were grown by the sitting drop vapor diffusion method at 20 °C in drops containing 1.5 μl of protein solution 1 (16 mg/ml) and 1 μl of reservoir 1 (100 mM MES, pH 6.5, 200 mM $(NH_4)_2SO_4$, and 30% (w/v) PEG 5000) or in drops containing 1.5 μl of protein solution 2 (16 mg/ml) and 1 μl of reservoir 2 (100 mM Tris-HCl, pH 8.5, and 2 M $(NH_4)_2SO_4$), respectively. Crystals with the space group *I*222 (form 1) grew in solution 1 with reservoir 1. Crystals with the space group *R*32 (form 2) grew in solution 2 with reservoir 2. M-RasP40D-GppNHp was dissolved in the buffer (50 mM Tris-HCl, pH 7.4, 50 mM NaCl, 5 mM $MgCl_2$, 1 mM EDTA, and 1 mM dithiothreitol). The crystals were grown by the sitting drop method at 20 °C in drops containing 2 μl of protein solution (18 mg/ml) and 2 μl of reservoir solution (28% (w/v) PEG 1500, 150 mM $MgSO_4$, and 100 mM sodium cacodylate, pH 6.5). M-RasP40D-GDP was dissolved in 50 mM Tris-HCl, pH 7.4, 100 mM NaCl, 5 mM $MgCl_2$, 1 mM EDTA, and 1 mM dithiothreitol. The crystals were grown by the sitting drop method at 20 °C in drops containing 2 μl of protein solution (20 mg/ml) and 2 μl of reservoir solution (20% (w/v) PEG 4000, 200 mM ammonium acetate, and 100 mM sodium acetate, pH 4.6). M-RasP40D/D41E/L51R-GppNHp was dissolved in 20 mM Tris-HCl, pH 8.0, 50 mM NaCl, 5 mM $MgCl_2$, 1 mM EDTA, and 1 mM dithiothreitol. The crystals were grown by the hanging drop method at 20 °C in drops containing 1 μl of protein solution (20 mg/ml) and 1 μl of reservoir solution (20% (w/v) PEG 4000, 160 mM $(NH_4)_2SO_4$, 80 mM sodium acetate, pH 5.20, and 10% (v/v) glycerol). After the crystals appeared in 24 h, they were crushed and used as microseeds for growing new crystals by the hanging drop method at 20 °C in drops containing 1 μl of protein solution (14 mg/ml) and 1 μl of reservoir solution (19% (w/v) PEG 4000, 160 mM $(NH_4)_2SO_4$, 80 mM sodium acetate, pH 5.20, and 10% (v/v) glycerol).

Data Collection and Structure Determination—The data collections at 100K were carried out at BL38B1 using Jupiter 210 (Rigaku Corp.) or Quantum 210 (ADSC) CCD detectors and at BL41XU using a Quantum 315 (ADSC) CCD detector in SPring-8. The data for H-RasT35S-GppNHp form 1 and form 2 were processed using the program HKL2000 (18), whereas those for M-RasP40D-GppNHp, M-RasP40D-GDP, and M-RasP40D/D41E/L51R-GppNHp were processed with the program MOSFLM (19) and scaled with the program SCALA in the CCP4 program suite (20). The crystal structures of H-RasT35S-GppNHp form 1 and form 2 were determined by the molecular replacement method with the program AMoRe (21) and MOLREP (22) by using H-RasWT-GppNHp (Protein Data Bank entry 5P21) as a search model. The structures of M-RasP40D-GppNHp, M-RasP40D-GDP, and M-RasP40D/

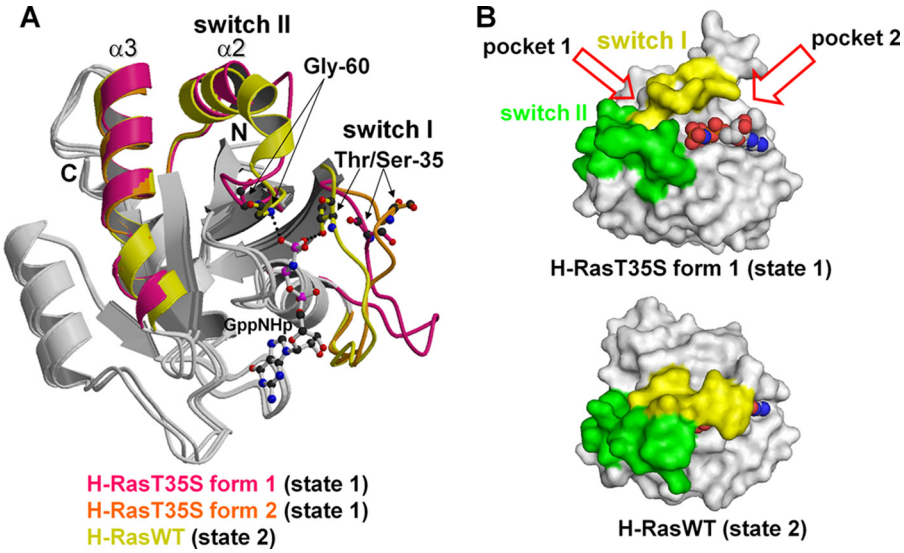

FIGURE 1. **Comparison of the crystal structures among H-RasT35S-GppNHp forms 1 and 2 and H-RasWT-GppNHp.** *A*, superimposition of the backbone structures of H-RasWT-GppNHp (*yellow*), H-RasT35S-GppNHp form 1 (*deep pink*), and H-RasT35S-GppNHp form 2 (*orange*). The structure of GppNHp is excerpted from the model of H-RasWT-GppNHp. The models were generated with Raster3D (27) and MOLSCRIPT (28) based on the least squares fittings of the overall residues excluding the invisible residues 61–71 of H-RasT35S-GppNHp form 2. GppNHp bound to H-RasWT and the side chains of the residues Thr/Ser-35 and Gly-60 for the H-Ras series are shown in a *ball-and-stick model* (*black*, carbon; *red*, oxygen; *blue*, nitrogen; *deep pink*, phosphorus). *B*, the surface models were generated by the program PyMOL (DeLano Scientific, LLC), where the two switch regions are highlighted (*yellow*, *switch I*; *green*, switch II). GppNHp is shown by a *CPK model*. The positions of the surface pockets found in H-RasT35S-GppNHp form 1 are shown by *red open arrows*.

D41E/L51R-GppNHp were determined in the same way using the structure of M-RasP40D-GDP (Protein Data Bank entry 3KKQ), M-RasWT-GDP (Protein Data Bank entry 1X1R) and M-RasWT-GppNHp (Protein Data Bank entry 1X1S) as search models, respectively. After the obtained model of each Ras was refined with the programs CNS (23) and REFMAC (24), it was corrected with a $2F_o - F_c$ map using the program COOT (25). Data collection and refinement statistics are summarized in supplemental Table 1.

Calculation of the γ-Phosphate Positional Changes and the Pocket Size—The program CONTACT in the CCP4 program suite (20) was used to search for the residues directly contacting with GppNHp via hydrogen bonding and/or van der Waals interaction in M-RasWT, M-RasP40D, M-RasP40D/D41E/L51R, H-RasWT, H-RasT35S form 1, and H-RasG60A. 13–20 residues were identified in each Ras protein, among which 12 residues (hereafter called reference residues) were conserved. The distance between the γ-phosphate positions of M-RasWT-GppNHp and M-RasP40D/D41E/L51R-GppNHp was measured after the least squares fitting of their reference residues by the program LSQKAB in the CCP4 program suite (20), and the r.m.s. deviation values of the Cα atoms of the reference residues were calculated. Similar calculations of the γ-phosphate distances and the r.m.s. deviation values of the Cα atoms of the reference residues were done with the pairs of M-RasWT-GppNHp and M-RasP40D-GppNHp, of H-RasWT-GppNHp and H-RasT35S-GppNHp form 1, and of H-RasWT-GppNHp and H-RasG60A-GppNHp. The volume of the surface pockets of H-RasT35S-GppNHp form 1 was calculated based on their crystal structures using the program MOE as described (see the Chemical Computing Group site on the World Wide Web).

Protein Data Bank codes of the coordinates used in the figures and tables are as follows: M-RasWT-GppNHp, 1X1S; M-RasWT-GDP, 1X1R; M-RasP40D-GppNHp, 3KKP; M-RasP40D-GDP, 3KKQ; M-RasP40D/D41E/L51R-GppNHp, 3KKO; H-RasWT-GppNHp, 1CTQ; H-RasWT-GDP, 4Q21; H-RasG60A-GppNHp, 1XCM; H-RasT35S-GppNHp form 1, 3KKN; H-RasT35S-GppNHp form 2, 3KKM; Rap2A-GTP, 3RAP chain R.

RESULTS

Two Distinct State 1 Crystal Structures of H-RasT35S-GppNHp and Their Implication in State 2 to State 1 Transition—Because crystallization of the state 1 conformer of the GppNHp-bound H-RasWT had been unsuccessful, we went over to solving the crystal structure of H-RasT35S-GppNHp. We thought this mutant might represent the intrinsic property of the state 1 structure of RasWT because it has a conservative substitution in Thr-35, the residue whose interaction with the γ-phosphate constitutes a key structural basis for the state transition. Moreover, the GppNHp-bound form of this mutant had been shown by ^{31}P NMR to predominantly adopt state 1 (10). A past attempt to solve the crystal structure of H-RasT35S-GppNHp had failed to identify the electron density of both the switch I and switch II regions (10). We made use of improved crystallization conditions, whose main differences were the replacement of 24% PEG 1500 (10) with 30% PEG 5000 or 2 M $(NH_4)_2SO_4$ as precipitants (see "Experimental Procedures" and Ref. 6 for the detailed conditions) and obtained two types of crystals with space groups *I*222 and *R*32, from which distinct tertiary structures were derived (supplemental Table 1). The electron density of the two switch regions in the H-RasT35S-GppNHp structure with the *I*222 space group (form 1) was completely clear, whereas the switch II residues 61–71 were invisible in the $2F_o - F_c$ electron density map of the structure with the *R*32 space group (form 2). Both form 1 and form 2 corresponded to state 1 as evidenced by the loss of the Ser-35-γ-phosphate interaction and marked deviation of the switch I loop from GppNHp, whereas the rest of the structure superimposed very well with that of H-RasWT-GppNHp state 2 (Protein Data Bank code 1CTQ) (Fig. 1*A*). Thus, form 1 represents the first complete state 1 structure of H-Ras-GppNHp. In addition, the switch II region of form 1 showed a conformation (a short α2-helix and a long loop) distinct from that of H-RasWT-GppNHp (a long α2-helix and a short loop) (Fig. 1*A*). Intriguingly, form 1 possessed a surface pocket (hereafter called pocket 1) between the two switch regions, which is similar to that found in M-Ras-GppNHp state 1 (15) (Fig. 1*B*). Moreover, it possessed a second pocket (hereafter called pocket

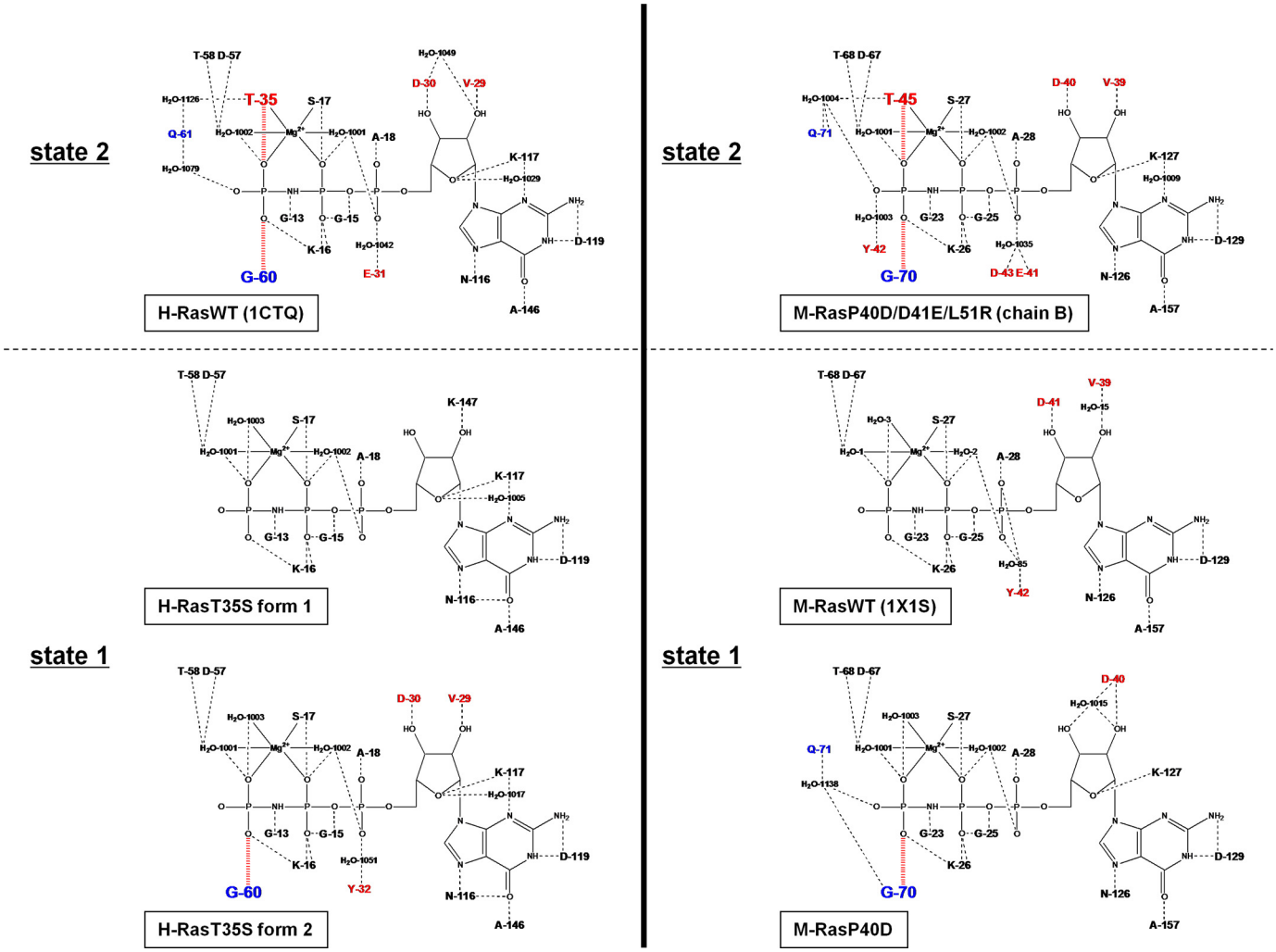

FIGURE 2. **Comparison of the hydrogen bonding networks of the nucleotide binding site.** Hydrogen bonding networks surrounding GppNHp of M-RasWT, H-RasWT, and their mutants are schematically shown together with Mg^{2+} and water molecules involved. The switch I and its N-terminal flanking residues are shown in *red*, and the switch II residues are shown in *blue*. The *dotted lines* represent hydrogen bonding interactions with a distance of less than 3.3 Å between donor and acceptor atoms, regardless of whether main chains or side chains of the residues are involved. The distance was calculated by using the program COOT (25).

2) between the switch I-flanking residues 28–31 and GppNHp. These pockets were unseen in the state 2 structure of H-RasWT-GppNHp (Fig. 1*B*). Form 2 did not have an equivalent of pocket 2 of form 1, and the existence of a pocket 1 equivalent remained unclear because of the complete loss of the electron density corresponding to the switch II residues 61–71, constituting a main part of the pocket edge. Superimposition of the two forms revealed the existence of prominent polysterism in the switch I loop; the r.m.s. deviation of Cα atoms of the switch I residues was 2.51 Å. Such polysterism was never observed in state 2 conformers; the corresponding r.m.s. deviation was 0.38 Å even between different proteins H-RasWT-GppNHp (Protein Data Bank code 1CTQ) and Rap2A-GppNHp (Protein Data Bank code 3RAP).

The discovery of the state 1-specific pockets and the switch I polysterism in H-RasT35S-GppNHp prompted us to investigate the intrinsic properties of the state 1 conformation through detailed comparison of the hydrogen bonding networks of the nucleotide binding site among the two state 1 conformers of H-RasT35S-GppNHp and the state 2 conformers of H-RasWT-GppNHp and Rap2A-GppNHp (Figs. 2 and 3*A* and supplemental Fig. 1). In the state 2 conformers, their switch I and switch II loops were stably fixed to the γ-phosphate via Thr-35 and Gly-60, respectively (7, 26). In striking contrast, the switch I loops of the both forms of H-RasT35S-GppNHp were not fixed to GppNHp due to the loss of the Ser-35-γ-phosphate interaction, causing deviation away from GppNHp and conformational instability (Figs. 1*A* and 3*A*). Moreover, in form 1, showing marked deviation of the switch I loop (Fig. 1*A*, *deep pink*), switch I-flanking Val-29 and Asp-30 and switch II Gly-60 failed to interact with the ribose and γ-phosphate of GppNHp, respectively (Figs. 2 and 3*A*). By contrast, in form 2, showing moderate deviation of the switch I loop, these interactions were fully restored, as was the case with H-RasWT-GppNHp (Figs. 1*A* (*orange*) and 2). However, the fact that the electron density of residues 61–71 was missing in form 2 implied that the switch II loop is highly mobile and not stably fixed to the γ-phosphate via Gly-60 even in this form. The instability of switch II in state 1 was also observed in the M-RasWT-GppNHp structure (15). Thus, in addition to the high flexibility

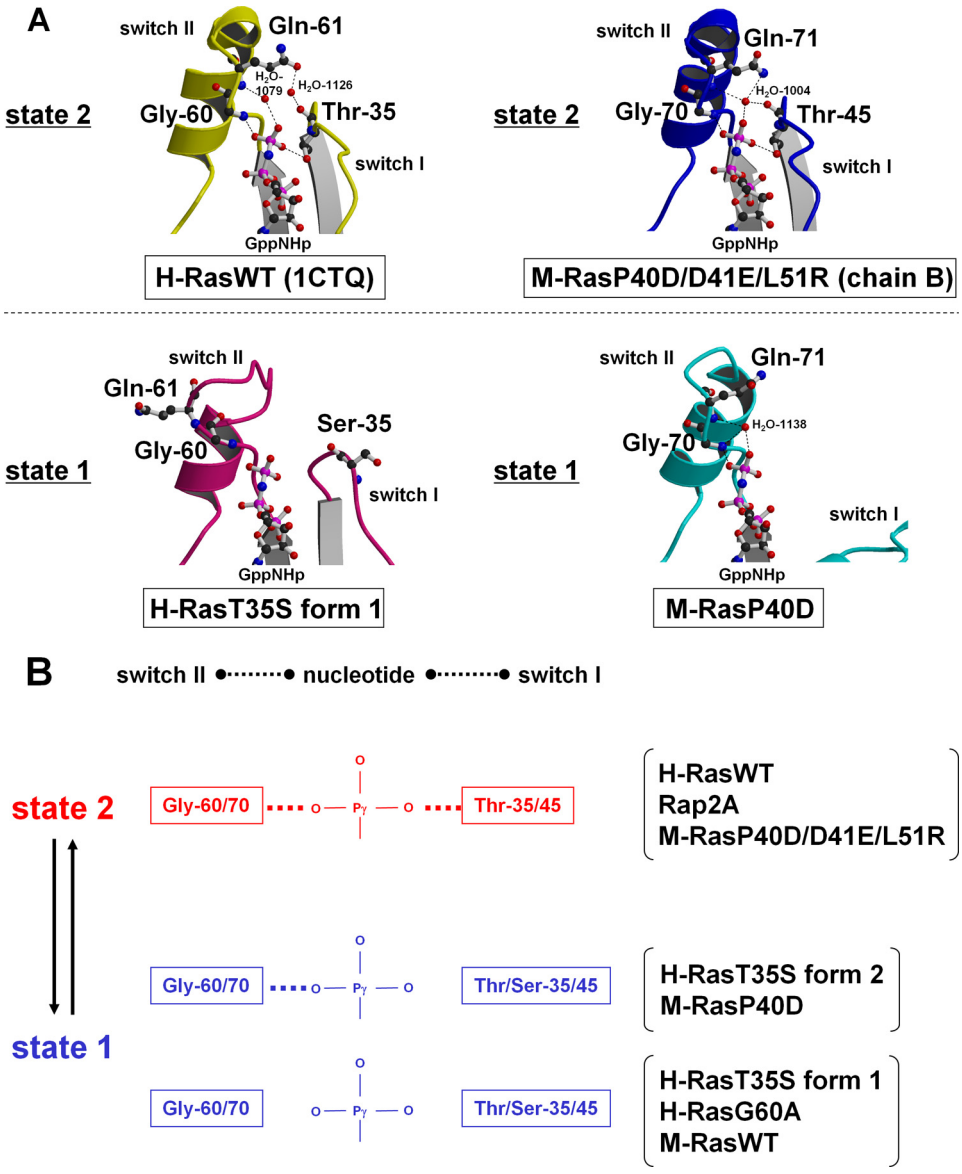

FIGURE 3. **Nucleotide γ-phosphate-mediated and water-mediated interactions between the switch I and switch II regions of H-Ras, M-Ras, and their mutants.** *A*, interactions between the two switch regions of the indicated proteins mediated by the γ-phosphate and water molecules are shown, where hydrogen bonds are indicated by *broken lines*. The main chains and side chains of Thr-35, Gly-60, and Gln-61 of H-RasWT and H-RasT35S form 1, Thr-45, Gly-70, and Gln-71 of M-RasP40D/D41E/L51R and M-RasP40D, and the bridging water molecules are shown in the *ball-and-stick model* (*black*, carbon; *red*, oxygen; *blue*, nitrogen; *deep pink*, phosphorus). The models were generated as described in the legend to Fig. 1*A*. *B*, γ-phosphate-mediated interactions between the switch I and switch II regions involving Thr-35/45 and Gly-60/70 (H-Ras/M-Ras) of H-Ras, M-Ras, and their mutants are schematically shown.

of switch I and its flanking region caused by the dissociation of Thr-35 from the nucleotide, the instability of switch II caused by the dissociation of Gly-60 from the nucleotide represents a common structural feature of state 1 distinguishing it from state 2. It must be emphasized that a single mutation T35S in switch I caused switch II instability and that both switch I and switch II underwent markedly different conformational changes between the two forms of H-RasT35S-GppNHp. These results suggest the existence of strong interdependency between the conformations of the two switch loops, which is mediated by the guanine nucleotide triphosphate. Moreover, the interdependence is strengthened by water-mediated interaction between the two switch loops in state 2, which is formed between Thr-35 in switch I and Gln-61 in switch II of H-RasWT and Rap2A, with H_2O-1126 and H_2O-30 acting as bridges, respectively (Figs. 2 and 3*A* and supplemental Fig. 1). This water-bridged interaction is lost in the state 1 conformers, such as form 1, which may also contribute to the instability of the switch loops.

These results suggested that the transition from state 2 to state 1 involves the dissociation of the two switch loops from GppNHp, which is mainly contributed by the dissociation of Thr-35 and Gly-60 from the γ-phosphate (Fig. 3*B*). This mechanism is supported by past electron spin resonance studies on the Mg^{2+}-binding site of H-Ras, showing the transient nature of the coordination of Thr-35 with the γ-phosphate (16, 17).

Identification of Amino Acid Residues Affecting the Conformational Equilibrium—M-Ras and H-Ras exhibit a high degree of overall sequence homology and possess identical switch I residues (supplemental Fig. 2), thereby sharing some of the effectors, guanine nucleotide exchange factors, and GTPase-activating proteins with each other (29, 30). However, they exhibit quite different state distribution in the GTP-bound forms; the state 1 population occupies 93 ± 2% for M-Ras-GppNHp and 36 ± 2% for H-Ras-GppNHp (7, 15). Because the T35S mutation was found useful in investigating the molecular basis of the transition toward state 1 in H-Ras, we searched for amino acid substitutions of M-Ras, which could induce the equilibrium shift toward state 2. Regarding the crucial role of the two switch regions in state transition, we focused on the differences in the residues flanking the identical switch I region between M-Ras and H-Ras, in particular Pro-40, Asp-41, and Leu-51 of M-Ras, corresponding to Asp-30, Glu-31, and Arg-41 of H-Ras, respectively, and in the switch II residues, in particular Phe-74 and Glu-79 of M-Ras, corresponding to Tyr-64 and Asp-69 of H-Ras, respectively (supplemental Fig. 2). Accordingly, we introduced P40D, D41E, and L51R mutations alone or in combinations into M-Ras, and the resulting mutant polypeptides in complex with GppNHp were examined for state distribution by ^{31}P NMR spectroscopy. The γ-phosphate resonance line in the spectrum of M-RasP40D-GppNHp showed a small but signifi-

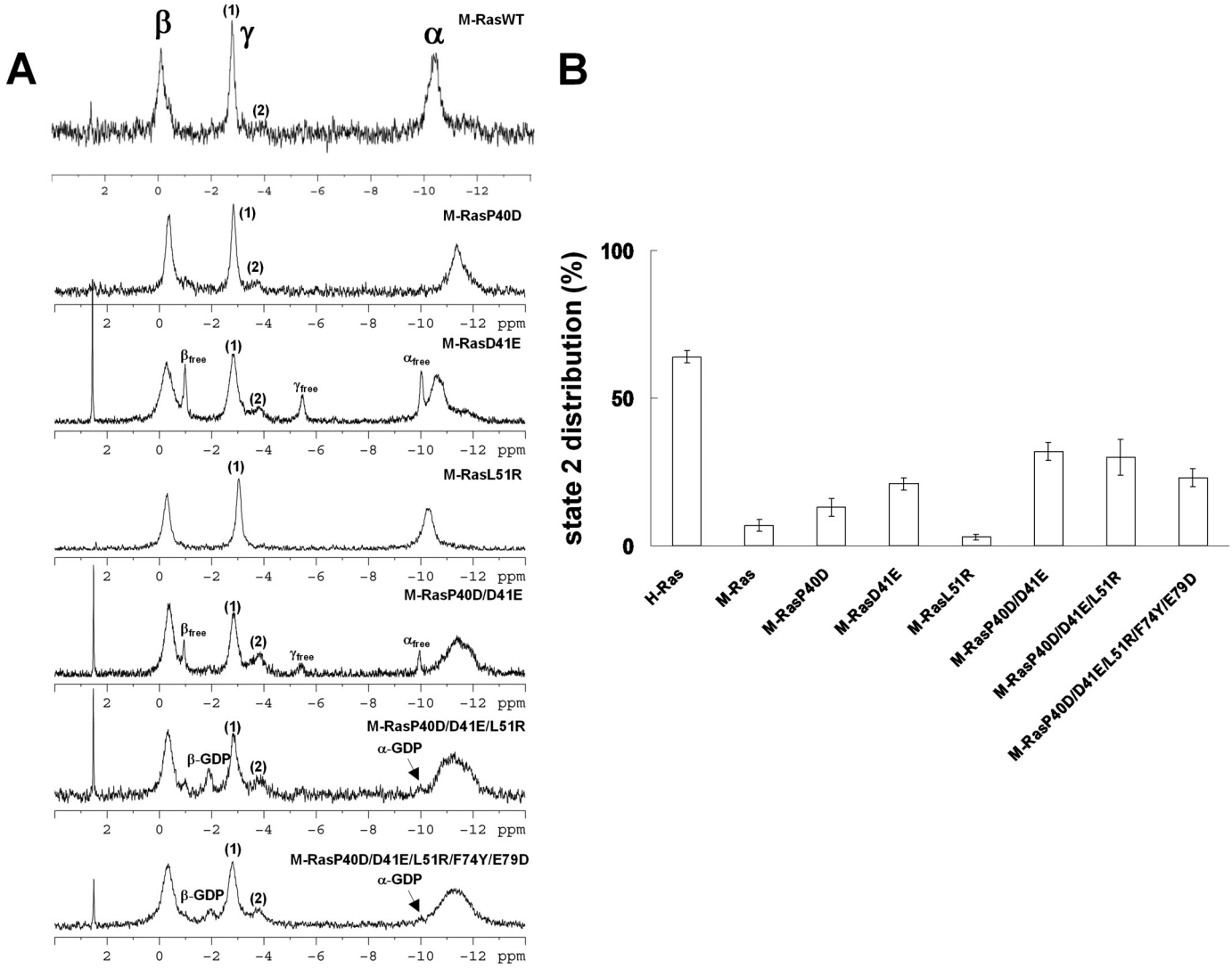

FIGURE 4. **^{31}P NMR spectra of various M-Ras mutants in complex with GppNHp.** *A*, the spectra were recorded using 1 mM solution of the indicated M-Ras mutant proteins. The spectrum of M-RasWT-GppNHp, adapted from Ref. 15, is shown as a control. α, β, and γ represent the α-, β- and γ-phosphate resonances, respectively. (*1*) and (*2*) represent the conformers in state 1 and state 2, respectively. α_{free}, β_{free}, and γ_{free} represent the α-, β- and γ-phosphate resonances of the free GppNHp, respectively. *α-GDP* and *β-GDP* represent the α- and β-resonances of GDP bound to M-Ras mutants, respectively. *B*, the state 1 and state 2 peaks in the γ-phosphate resonance of each GTPase were fitted by Lorentz curves, and the state 1 proportion was calculated as [state 1]/([state 1] + [state 2]), where [state 1] and [state 2] represent the relative concentrations obtained as the integrals of the corresponding peaks. *Error bars*, standard deviations derived from the Lorentz curve fitting.

cant increase of the state 2 population (at −3.75 ppm) to 13 ± 3% compared with that (at −3.9 ppm) of M-RasWT-GppNHp (7 ± 2%) (Fig. 4, *A* and *B*, and supplemental Table 2). The state assignment of the two peaks of the γ-phosphate resonance line was confirmed by transition of the −2.9 ppm peak to the −3.75 ppm peak by the addition of c-Raf-1 Ras-binding domain (supplemental Fig. 3). M-RasD41E-GppNHp showed a higher increase of the state 2 population, reaching 21 ± 2%. In contrast, the L51R mutation showed no effect. Further, examination of the combinatorial effects of the mutations revealed that the state 2 population of M-RasP40D/D41E-GppNHp increased to 32 ± 3%, which was unaffected by the addition of the L51R mutation. Likewise, the addition of both the F74Y and E79D mutations to M-RasP40D/D41E/L51R showed no additional effect on the state distribution (Fig. 4, *A* and *B*, supplemental Tables 2 and 3, and supplemental Fig. 3). These results indicated that both Pro-40 and Asp-41 of M-Ras play crucial roles in stabilizing state 1 conformation.

Crystal Structures of M-RasP40D-GppNHp and M-RasP40D/D41E/L51R-GppNHp and Their Implication in State 1 to State 2 Transition—Hoping to obtain structural information pertinent to the state 1 to state 2 transition, the M-Ras mutants with increased populations of state 2 were subjected to crystal structure analyses in their GppNHp-bound forms. Eventually, we succeeded in solving the structures of M-RasP40D-GppNHp and M-RasP40D/D41E/L51R-GppNHp (supplemental Table 1), both of which superimposed very well with those of M-RasWT-GppNHp (Protein Data Bank code 1X1S) and H-RasWT-GppNHp (Protein Data Bank code 1CTQ) except for the two switch regions (Fig. 5*A*). The hydrogen bonding networks of the nucleotide binding sites are illustrated in Fig. 2. M-RasP40D adopted a state 1 conformation, as characterized by dissociation of

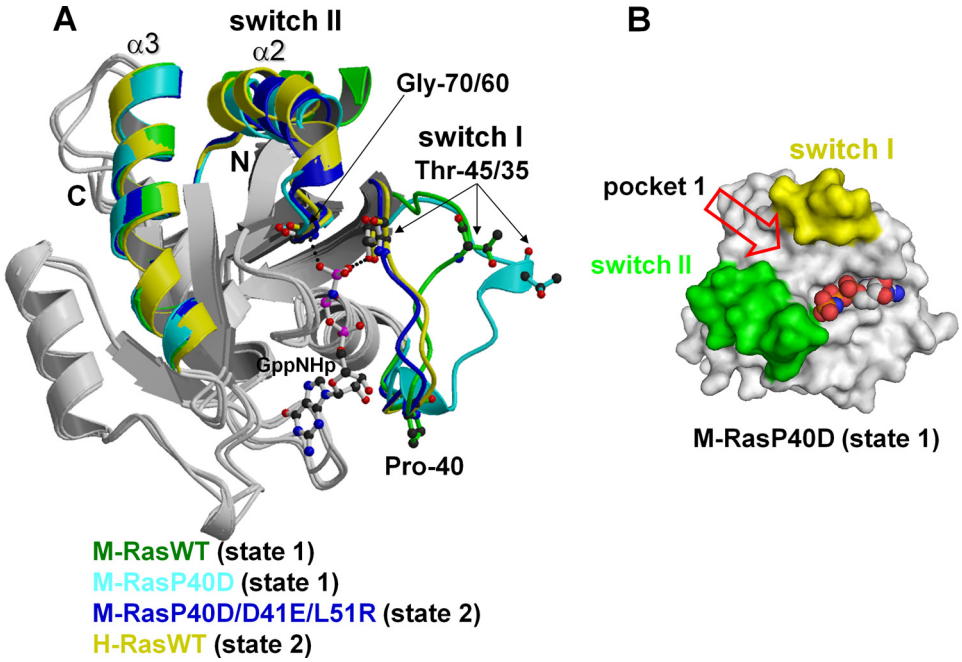

FIGURE 5. **Comparison of the crystal structures among the GppNHp-bound forms of M-RasWT, M-RasP40D, M-RasP40D/D41E/L51R, and H-RasWT.** *A*, superimposition of the backbone structures of M-RasWT-GppNHp (*green*), M-RasP40D-GppNHp (*cyan*), M-RasP40D/D41E/L51R-GppNHp (*blue*), and H-RasWT-GppNHp (*yellow*). The structure of GppNHp is excerpted from the model of M-RasP40D/D41E/L51R-GppNHp. The models were generated as described in the legend to Fig. 1*A* excluding the invisible residues 69–73 of M-RasWT. *B*, the surface models were generated as described in the legend to Fig. 1*B*. The position of the surface pocket found in M-RasP40D is shown by a *red open arrow*.

the Thr-45-γ-phosphate interaction and marked deviation of the switch I loop (Fig. 3*A*). Because the electron density of the switch II residues, missing in the M-RasWT-GppNHp structure (15), was well resolved, this represented the first complete M-Ras state 1 structure with a high resolution of 1.35 Å. It possessed a surface pocket corresponding to pocket 1 of H-RasT35S form 1 but not a second pocket corresponding to pocket 2 (Fig. 5*B*). As shown in Fig. 2, the hydrogen bonding network of the residues 39–42 with the ribose and α-phosphate was rearranged from those of M-RasWT-GppNHp; Asp-40 restored the contact with the hydroxyl group of the ribose, similar to the case with H-RasWT-GppNHp, and Asp-41 lost the contact with the nucleotide. Another major difference from M-RasWT-GppNHp was the establishment of a direct interaction of Gly-70 with the γ-phosphate of GppNHp, which resulted in stabilization of the switch II loop on the nucleotide similar to the case with H-RasWT-GppNHp (Figs. 2 and 3*A*). Thus, the P40D mutation in switch I resulted in stabilization of the flexible switch II region mainly through establishment of the Gly-70-γ-phosphate interaction, leading to an increase of the state 2 population.

On the other hand, the crystal structure of M-RasP40D/D41E/L51R-GppNHp corresponded to state 2 as evidenced by the switch I loop stabilization on the nucleotide via direct and Mg^{2+}-coordinated indirect interactions of Thr-45 with the γ-phosphate of GppNHp (Figs. 2 and 3*A*). Although this is rather unexpected considering the minority of state 2 (<50%) in solution (Fig. 4*B* and supplemental Table 2), similar phenomena have been observed for a couple of other H-Ras mutants (4, 11) and probably reflect preferential crystallization of conformationally stabler forms. Like M-RasP40D-GppNHp, the switch II loop of M-RasP40D/D41E/L51R-GppNHp was stabilized to the nucleotide via an interaction of Gly-70 with the γ-phosphate (Fig. 3*A*). Further, the hydrogen bonding network of the switch I and its flanking residues of this mutant bore close resemblance to that of H-RasWT-GppNHp; both Asp-40 and Val-39 made direct contacts with the hydroxyl groups of the ribose, and Glu-41 formed a water-mediated interaction with the α-phosphate (Fig. 2). Consequently, the backbone structure of the two switch regions of M-RasP40D/D41E/L51R-GppNHp superimposed very well with that of H-RasWT-GppNHp (Fig. 5*A*). Moreover, the two switch loops of M-RasP40D/D41E/L51R-GppNHp established a water-mediated interaction, with H_2O-1004 acting as a bridge between Thr-45 in switch I and Gln-71 in switch II, like the cases with H-RasWT-GppNHp and Rap2A-GppNHp (Figs. 2 and 3*A* and supplemental Fig. 1).

The results obtained with the M-Ras mutants confirmed the structural features distinguishing the two states, which were revealed by the study on H-RasT35S form 1 and form 2. Also, they suggested that the transition from state 1 to state 2 involves the association of the two switch loops with GppNHp via achievements of the interaction of Thr-45 and Gly-70 with the γ-phosphate. The important role of the nucleotide-mediated interdependence between the two switch loops in undergoing such structural changes was further supported by the fact that a single switch I mutation, P40D, caused restoration of the Gly-70-γ-phosphate interaction in switch II. Moreover, the facilitative role of the water-bridged interaction between the two switch loops in state 2 formation gained further support from the result on M-RasP40D/D41E/L51R-GppNHp.

Crucial Role of the Nucleotide Positional Change in State Transition—The results obtained so far comprehensively indicated that the state transition is caused by rearrangement of the hydrogen bonding networks of the nucleotide binding site, where the switch I and switch II regions exhibit strong interdependence mediated by the guanine nucleotide via Thr-35/45 and Gly-60/70 (Fig. 3*B*). This led us to examine the positional or conformational change of the guanine nucleotide accompanying the state transition and its effect on the switch region conformation.

The crystal structures of H-RasT35S-GppNHp could be regarded as intermediates reflecting a facet of the conformational changes along the path from state 2 to state 1 (Fig. 6*A*). Because the switch II region was missing in H-RasT35S-GppNHp form 2, we used form 1 only for the following analysis. As shown in Fig. 6*A*, the γ-phosphate position exhibited a

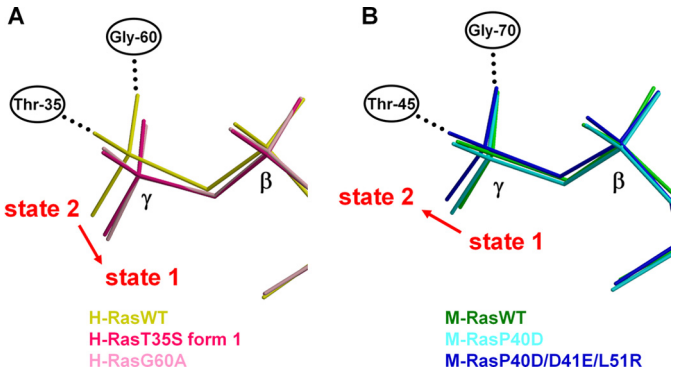

FIGURE 6. **Positional changes of the γ-phosphate accompanying the state transition.** *A*, the positions of the β- and γ-phosphates of GppNHp relative to the reference residues (see "Experimental Procedures") are shown: H-RasWT (*yellow*), H-RasG60A (*pink*), and H-RasT35S form 1 (*deep pink*). The direction of the positional change of the γ-phosphate accompanying the state 2 to state 1 transition is indicated by a *red arrow*. *B*, the positions of the β- and γ-phosphates of GppNHp relative to the reference residues (see "Experimental Procedures") are shown: M-RasWT (*green*), M-RasP40D (*cyan*), and M-RasP40D/D41E/L51R (*blue*). The direction of the positional change of the γ-phosphate accompanying the state 1 to state 2 transition is indicated by a *red arrow*. β and γ represent the β- and γ-phosphate, respectively.

change of ~0.46 Å for H-RasT35S-GppNHp compared with H-RasWT-GppNHp in the direction away from Thr-35 and Gly-60, which was a significant value, considering the value of r.m.s. deviation of Cα atoms of reference residues (see "Experimental Procedures"), 0.12 Å. Apparently, there is a causal relationship between this γ-phosphate positional change and the loss of the interactions between the two switch loops and the nucleotide. In the case of H-RasT35S-GppNHp, the loss of a side chain methyl group of Thr-35 facilitates the dissociation of this residue from the γ-phosphate, resulting in dissociation of the switch I loop from the nucleotide. The dissociation causes a positional change of the nucleotide (Fig. 6*A*), leading to dissociation of Gly-60 from the γ-phosphate (Figs. 2 and 3*A*). It should be noted that residues other than Thr-35 and Gly-60, such as the switch I-flanking residues, which are involved in rearrangement of the hydrogen bonding networks of the nucleotide binding site, may also play a role for the state transition (Fig. 2). Through extensive searches of the literature and the Protein Data Bank, we found that the reported structures of H-RasG60A-GppNHp and H-RasG60A/K147A (31, 32) might correspond to state 1, although the authors did not attempt to make state assignment for these mutants by ^{31}P NMR in the presence of the effectors. This assumption was based on the loss of the Thr-35-γ-phosphate interaction and marked deviation of the switch I loop away from GppNHp in their structures. Also, the backbone structures of the two switch regions of these mutants along with the side chain of Phe-28, showing prominent deviation form the nucleotide, superimposed well with those of H-RasT35S-GppNHp form 1 except for the N-terminal region of switch I (supplemental Fig. 5). If this is the case, H-RasG60A-GppNHp represents an example of a switch II mutation causing the switch I conformational change, providing a further support for the importance of the nucleotide-mediated interdependence between the two switch regions. Moreover, H-RasG60A-GppNHp exhibits a γ-phosphate positional shift of ~0.47 Å (*cf.* r.m.s. deviation of Cα atoms of reference residues: 0.15 Å) in the direction approaching Thr-35 and Gly-60 compared with H-RasWT-GppNHp (Fig. 6*A*).

In a similar vein, the path from state 1 to state 2 could be traced by using a series of the crystal structures of M-RasWT, M-RasP40D, and M-RasP40D/D41E/L51R in complex with GppNHp (Fig. 6*B*). Comparison of the γ-phosphate position between M-RasWT-GppNHp and M-RasP40D/D41E/L51R-GppNHp revealed a change of ~0.25 Å in the direction approaching Thr-45 and Gly-70 (Fig. 6*B*), where the r.m.s. deviation of Cα atoms of reference residues was 0.10 Å. This positional change is probably initiated by rearrangement of the hydrogen bonding between the residues 40/41 and the ribose/α-phosphate of GppNHp due to the mutations (Fig. 2 and supplemental Fig. 4). The establishment of the γ-phosphate interaction with both Gly-70 and Thr-45 seems to be necessary for attaining the observed change of the γ-phosphate position because M-RasP40D failed to show a significant change (Fig. 6*B*), where the values for the γ-phosphate positional change and for the r.m.s. deviation of Cα atoms of reference residues were 0.14 Å and 0.12 Å, respectively.

DISCUSSION

State Transition Mechanisms Inferred from Crystal Structures of State Intermediates—Conformational equilibrium between the two states is shared over diverse members of the small GTPase family in their GTP-bound forms (5, 33). However, the molecular basis for this equilibrium remained largely unknown mainly due to the scarcity of structural information on state 1 and state intermediates. Also, the extremely slow equilibrium velocity on the order of 10^{-3} s precluded a molecular dynamics simulation to predict a path for the state transition based on the existing structural information. In this paper, we are able to trace the conformational changes along the path through the crystal structure analyses of a series of mutant H-Ras and M-Ras proteins, which can be regarded as intermediates of the state transition.

Comparison of the various crystal structures representing state 1 or state 2 reveals the structural features favoring state 2 formation (Fig. 3*B*), stabilization of the switch I and switch II loops to the nucleotide through interaction of Thr-35/45 and Gly-60/70 (H-Ras/M-Ras) with the γ-phosphate. Moreover, discovery of the regional polysterism in the two switch regions of H-RasT35S form 1 and form 2 (Fig. 1*A*), along with the conformational change of switch II in M-RasP40D (Fig. 5*A*), reveal a crucial role of the nucleotide-mediated interdependence between the two switch regions in the state transition, which is influenced by a water-mediated bridge formation between the two switch loops. Furthermore, our results indicate that the positional change of the nucleotide γ-phosphate is intimately involved in the nucleotide-mediated interaction between the two switch regions (Fig. 6).

Proposal of Common Mechanistic Basis between State Transition and GDP/GTP Exchange—High flexibility is a main feature of the two switch regions of Ras, which enables conformational transition associated with a GDP/GTP exchange (3, 26). Our present results lead us to deduce that the dynamic equilibrium of Ras-GTP may also be generated by this property of the switch regions. Comparison between the conformational

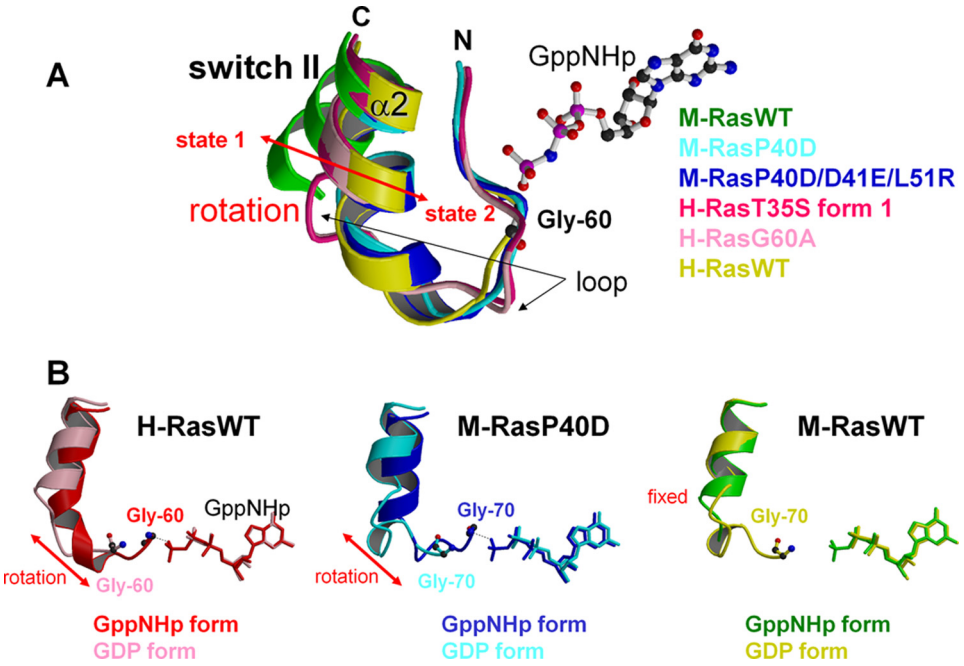

FIGURE 7. **Structural features of the switch II regions and their changes accompanying the GDP/GTP exchange.** *A*, superimposition of the backbones of the switch II residues (60–75 for H-Ras and 70–85 for M-Ras) of M-RasWT-GppNHp (*green*), M-RasP40D-GppNHp (*cyan*), M-RasP40D/D41E/L51R-GppNHp (*blue*), H-RasWT-GppNHp (*yellow*), H-RasT35S-GppNHp form 1 (*deep pink*), and H-RasG60A-GppNHp (*pink*). The structures of GppNHp and Gly-60 are excerpted from the model of H-RasWT-GppNHp and are shown in a *ball-and-stick model*. *B*, the switch II structures and the nucleotide positions were compared between the GDP-bound and GppNHp-bound forms by superimposition of the corresponding regions of H-RasWT (GDP-bound form in *pink* and GppNHp-bound form in *red*), M-RasP40D (GDP-bound form in *cyan* and GppNHp-bound form in *blue*), and M-RasWT (GDP-bound form in *yellow* and GppNHp-bound form in *green*). Gly-60/70 is shown in a *ball-and-stick model*. The models were generated as described in the legend to Fig. 1*A*.

changes upon the GDP/GTP and state 1/state 2 transitions reveals the existence of a common interesting feature as follows. The switch II loop of the state 1 conformers, such as H-RasT35S-GppNHp form 1 and possibly H-RasG60A-GppNHp, is longer than that of the state 2 conformers, such as H-RasWT-GppNHp and M-RasP40D/D41E/L51R-GppNHp, because the C-terminal part of the loop is stabilized and remodeled into an α-helix through direct interaction of Gly-60/70 with the γ-phosphate in the state 2 conformers (Fig. 7*A*). Concomitantly, the α2-helix of the state 2 conformers exhibits significant rotation toward the α3-helix compared with the state 1 conformers (Figs. 1*A* and 5*A*). Similar switch II conformational changes are observed in the GDP/GTP exchange cycle. The switch II region of H-RasWT-GDP (Protein Data Bank entries 4Q21 and 1Q21), whose Gly-60 fails to interact with GDP, consists of a longer loop and a shorter α-helix compared with that of the H-RasWT-GppNHp (1CTQ) (Fig. 7*B*). In another crystal of H-RasWT-GDP (Protein Data Bank entry 1IOZ), the electron density of a part of the switch II loop is completely missing, suggesting its high flexibility. Indeed, NMR spectra of H-RasWT-GDP (Protein Data Bank entries 1CRP and 1CRR) showed remarkable flexibility in this region. Upon nucleotide exchange from GDP to GTP/GppNHp, a gain of γ-phosphate causes the stabilization of the switch II loop to the nucleotide mainly via establishment of the Gly-60-γ-phosphate interaction, which results in remodeling of the C-terminal part into an α-helix (3, 26) (Fig. 7*B*). This model is supported by the observation that M-RasWT-GppNHp, which predominantly adopts state 1 and lacks the Gly-60-γ-phosphate interaction in its GppNHp-bound form, fails to undergo the switch II conformational changes upon the GDP/GTP exchange (Fig. 7*B*). In a similar vein, M-RasP40D-GppNHp, which restores the Gly-60-γ-phosphate interaction in its GppNHp-bound form, undergoes a switch II conformational change upon the GDP/GTP exchange (Fig. 7*B*). These results collectively demonstrate that the highly flexible property of the two switch regions, especially switch II, is responsible for both the GDP/GTP and state 1/state 2 transitions, which is mediated by the positional changes of the γ-phosphate.

The State 1-specific Pockets as a Promising Target for the Development of Ras Inhibitors—The dramatic effect of Imatinib (Gleevec of Novartis) (34), targeting the oncogene product Abl, on chronic myelogenous leukemia has boosted hopes for the molecular approach to cancer therapy (*i.e.* the development of anti-cancer drugs targeting the oncogene products). However, Ras has been refractory to this approach, although it is one of the most attractive anti-cancer drug targets (1). Also, the activated Ras is known to cause "oncogene addiction" in cancer cells carrying it (35), implying that its pharmacological inhibition leads to cell death. In this study, we discover surface pockets on the state 1 structure of H-Ras-GTP, which are unseen in the state 2 or H-Ras-GDP structure, through the x-ray crystallographic analysis of H-RasT35S-GppNHp form 1. The pockets of H-RasT35S-GppNHp form 1 seem to be a promising target for the structure-based drug design of Ras inhibitors for the following reasons. First, compounds fitting into this state 1-specific pocket are predicted to inhibit Ras function by holding it in the state 1 "inactive" conformation. This notion is supported by the fact that activated Ras mutants, such as H-RasG12V and H-RasQ61L, also exhibit the same conformational equilibrium in their GppNHp-bound forms (4, 11). Further, very close resemblance between the pocket structures of H-RasT35S-GppNHp form 1 and H-RasG60A-GppNHp implies that a common and essential structural feature of the state 1 pocket of H-RasWT-GTP is represented by these structures. This is indeed backed by the fact that our crystal structure (2.2 Å)[4] of H-RasWT-GppNHp corresponding to state 1 reveals very close resemblance to that of H-RasT35S-GppNHp form 1, which is exemplified by loss of the Thr-35 and Gly-60 interactions with the γ-phosphate, and formation of two surface pockets with

[4] F. Shima, S. Muraoka, and T. Kataoka, unpublished data.

similar shapes. These results collectively suggest that the state 1 structures of the activated Ras mutants, although yet to be determined, are likely to adopt a similar conformation. Moreover, the cubic capacities of pocket 1 and pocket 2 (Fig. 1*B*) of H-RasT35S-GppNHp form 1 were calculated to be 328 and 568 $Å^3$, respectively, which are large enough to accommodate small molecule compounds. Furthermore, the size and shape of the pockets of H-RasT35S-GppNHp form 1 are obviously different from those of the pocket of M-RasP40D-GppNHp (Fig. 1*B* and 5*B*), indicating their high specificity among various Ras family GTPase species. Taking these results and information together, the structural information of the state 1-specific pockets will provide an invaluable tool for the structure-based drug design of Ras inhibitors based on computer docking screening.

In addition, our finding of the crucial role of the nucleotide-mediated interaction between the two switch regions may provide a new insight into the target site selection for the development of Ras inhibitors; compounds which interact with switch II and cause its instability may also be effective in inhibiting Ras functions through induction of a switch I conformational change. Further studies on the molecular basis for the state transition will provide us with invaluable resources for rational drug development targeting not only Ras but also other small GTPases.

Acknowledgments—The synchrotron radiation experiments were performed at BL38B1 and BL41XU in the SPring-8 with the approval of the Japan Synchrotron Radiation Research Institute (JASRI) (Proposals 2006A1786 and 2009A1102). We thank Masahide Kawamoto, Kazuya Hasegawa, Nobutaka Shimizu, Seiki Baba, and Nobuhiro Mizuno of JASRI/SPring-8 for data collection in the SPring-8 and for technical advice. We thank Tomoko Inoue for excellent technical assistance. We thank Dr. Hidekazu Hiroaki of Kobe University for critically reading the manuscript.

REFERENCES

1. Downward, J. (2003) *Nat. Rev. Cancer* **3,** 11–22
2. Corbett, K. D., and Alber, T. (2001) *Trends. Biochem. Sci.* **26,** 710–716
3. Vetter, I. R., and Wittinghofer, A. (2001) *Science* **294,** 1299–1304
4. Geyer, M., Schweins, T., Herrmann, C., Prisner, T., Wittinghofer, A., and Kalbitzer, H. R. (1996) *Biochemistry* **35,** 10308–10320
5. Geyer, M., Assheuer, R., Klebe, C., Kuhlmann, J., Becker, J., Wittinghofer, A., and Kalbitzer, H. R. (1999) *Biochemistry* **38,** 11250–11260
6. Spoerner, M., Nuehs, A., Herrmann, C., Steiner, G., and Kalbitzer, H. R. (2007) *FEBS J.* **274,** 1419–1433
7. Liao, J., Shima, F., Araki, M., Ye, M., Muraoka, S., Sugimoto, T., Kawamura, M., Yamamoto, N., Tamura, A., and Kataoka, T. (2008) *Biochem. Biophys. Res. Commun.* **369,** 327–332
8. Fenwick, R. B., Prasannan, S., Campbell, L. J., Nietlispach, D., Evetts, K. A., Camonis, J., Mott, H. R., and Owen, D. (2009) *Biochemistry* **48,** 2192–2206
9. Linnemann, T., Geyer, M., Jaitner, B. K., Block, C., Kalbitzer, H. R., Wittinghofer, A., and Herrmann, C. (1999) *J. Biol. Chem.* **274,** 13556–13562
10. Spoerner, M., Herrmann, C., Vetter, I. R., Kalbitzer, H. R., and Wittinghofer, A. (2001) *Proc. Natl. Acad. Sci. U.S.A.* **98,** 4944–4949
11. Spoerner, M., Wittinghofer, A., and Kalbitzer, H. R. (2004) *FEBS Lett.* **578,** 305–310
12. Pai, E. F., Krengel, U., Petsko, G. A., Goody, R. S., Kabsch, W., and Wittinghofer, A. (1990) *EMBO J.* **9,** 2351–2359
13. Huang, L., Hofer, F., Martin, G. S., and Kim, S. H. (1998) *Nat. Struct. Biol.* **5,** 422–426
14. Pacold, M. E., Suire, S., Perisic, O., Lara-Gonzalez, S., Davis, C. T., Walker, E. H., Hawkins, P. T., Stephens, L., Eccleston, J. F., and Williams, R. L. (2000) *Cell* **103,** 931–943
15. Ye, M., Shima, F., Muraoka, S., Liao, J., Okamoto, H., Yamamoto, M., Tamura, A., Yagi, N., Ueki, T., and Kataoka, T. (2005) *J. Biol. Chem.* **280,** 31267–31275
16. Bellew, B. F., Halkides, C. J., Gerfen, G. J., Griffin, R. G., and Singel, D. J. (1996) *Biochemistry* **35,** 12186–12193
17. Halkides, C. J., Bellew, B. F., Gerfen, G. J., Farrar, C. T., Carter, P. H., Ruo, B., Evans, D. A., Griffin, R. G., and Singel, D. J. (1996) *Biochemistry* **35,** 12194–12200
18. Otwinowski, Z., and Minor, W. (1997) *Methods Enzymol.* **276,** 307–326
19. Leslie, A. G. W. (1992) *Joint CCP4 and ESF-EACBM Newsletter on Protein Crystallography*, No. 26, Daresbury Laboratory, Warrington, UK
20. Collaborative Computational Project Number 4 (1994) *Acta Crystallogr. D* **50,** 760–763
21. Navaza, J. (1994) *Acta Crystallogr. A* **50,** 157–163
22. Vagin, A., and Teplyakov, A. (1997) *J. Appl. Crystallogr.* **30,** 1022–1025
23. Brünger, A. T., Adams, P. D., Clore, G. M., DeLano, W. L., Gros, P., Grosse-Kunstleve, R. W., Jiang, J. S., Kuszewski, J., Nilges, M., Pannu, N. S., Read, R. J., Rice, L. M., Simonson, T., and Warren, G. L. (1998) *Acta Crystallogr. D* **54,** 905–921
24. Murshudov, G. N., Vagin, A. A., and Dodson, E. J. (1997) *Acta Crystallogr. D* **53,** 240–255
25. Emsley, P., and Cowtan, K. (2004) *Acta Crystallogr. D* **60,** 2126–2132
26. Cherfils, J., Ménétrey, J., Le Bras, G., Janoueix-Lerosey, I., de Gunzburg, J., Garel, J. R., and Auzat, I. (1997) *EMBO J.* **16,** 5582–5591
27. Merritt, E. A., and Murphy, M. E. P. (1994) *Acta Crystallogr. D* **50,** 869–873
28. Kraulis, P. J. (1991) *J. Appl. Crystallogr.* **24,** 946–950
29. Quilliam, L. A., Castro, A. F., Rogers-Graham, K. S., Martin, C. B., Der, C. J., and Bi, C. (1999) *J. Biol. Chem.* **274,** 23850–23857
30. Ohba, Y., Mochizuki, N., Yamashita, S., Chan, A. M., Schrader, J. W., Hattori, S., Nagashima, K., and Matsuda, M. (2000) *J. Biol. Chem.* **275,** 20020–20026
31. Ford, B., Skowronek, K., Boykevisch, S., Bar-Sagi, D., and Nassar, N. (2005) *J. Biol. Chem.* **280,** 25697–25705
32. Ford, B., Boykevisch, S., Zhao, C., Kunzelmann, S., Bar-Sagi, D., Herrmann, C., and Nassar, N. (2009) *Biochemistry* **48,** 11449–11457
33. Phillips, M. J., Calero, G., Chan, B., Ramachandran, S., and Cerione, R. A. (2008) *J. Biol. Chem.* **283,** 14153–14164
34. Fabbro, D., Ruetz, S., Buchdunger, E., Cowan-Jacob, S. W., Fendrich, G., Liebetanz, J., Mestan, J., O'Reilly, T., Traxler, P., Chaudhuri, B., Fretz, H., Zimmermann, J., Meyer, T., Caravatti, G., Furet, P., and Manley, P. W. (2002) *Pharmacol. Ther.* **93,** 79–98
35. Weinstein, I. B. (2002) *Science* **297,** 63–64